IOP PUBLISHING NANOTECHNOLOGY
Nanotechnology **18** (2007) 345202 (8pp) doi:10.1088/0957-4484/18/34/345202

All-inkjet-printed flexible electronics fabrication on a polymer substrate by low-temperature high-resolution selective laser sintering of metal nanoparticles

Seung H Ko[1], Heng Pan[1], Costas P Grigoropoulos[1,4], Christine K Luscombe[2], Jean M J Fréchet[2] and Dimos Poulikakos[3]

[1] Department of Mechanical Engineering, University of California, 6177 Etcheverry Hall, Berkeley, CA 94720-1740, USA
[2] Department of Chemistry, University of California, Berkeley, CA 94720-1460, USA
[3] Laboratory of Thermodynamics in Emerging Technologies, Department of Mechanical and Process Engineering, ETH Zurich, CH-8092 Zurich, Switzerland

E-mail: cgrigoro@me.berkeley.edu

Received 11 April 2007, in final form 15 June 2007
Published 1 August 2007
Online at stacks.iop.org/Nano/18/345202

Abstract
All-printed electronics is the key technology to ultra-low-cost, large-area electronics. As a critical step in this direction, we demonstrate that laser sintering of inkjet-printed metal nanoparticles enables low-temperature metal deposition as well as high-resolution patterning to overcome the resolution limitation of the current inkjet direct writing processes. To demonstrate this process combined with the implementation of air-stable carboxylate-functionalized polythiophenes, high-resolution organic transistors were fabricated in ambient pressure and room temperature without utilizing any photolithographic steps or requiring a vacuum deposition process. Local thermal control of the laser sintering process could minimize the heat-affected zone and the thermal damage to the substrate and further enhance the resolution of the process. This local nanoparticle deposition and energy coupling enable an environmentally friendly and cost-effective process as well as a low-temperature manufacturing sequence to realize large-area, flexible electronics on polymer substrates.

(Some figures in this article are in colour only in the electronic version)

1. Introduction

The development of electric circuit fabrication on polymer substrates has attracted significant interest as a pathway to low-cost or large-area electronics [1, 2]. The conventional vacuum deposition and photolithographic patterning methods are well developed for inorganic microelectronics. However, flexible polymer substrates are chemically incompatible with resists, etchants and developers used in conventional integrated circuit (IC) processing. In practice, conventional IC fabrication processes are subject to limitations in that they are multi-step, involve high processing temperatures and toxic waste and are therefore expensive. Furthermore, the increasing size of electronic devices such as displays poses great difficulty in adapting standard microfabrication processes, including lithographic patterning.

The high-resolution direct printing technique is of particular interest as an alternative to conventional vacuum deposition and photolithographic patterning of various functional films such as gate electrodes, gate dielectrics, source and drain contacts and active semiconductor layers [1]. Among direct printing techniques such as micro contact

[4] Author to whom any correspondence should be addressed.

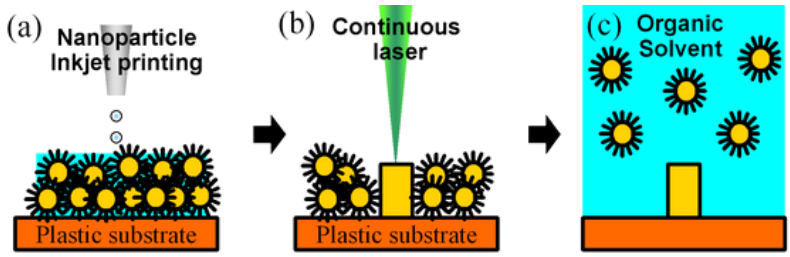

Figure 1. Selective laser sintering process of inkjet printed nanoparticle solution on a polymer substrate by scanning with a focused continuous laser. The circles represent Au nanoparticles with a self-assembled monolayer (SAM) and the square block indicates a conductor pattern of sintered gold nanoparticles. Unsintered nanoparticles are simply washed away in an organic solvent.

printing (μ-CP) [1, 3, 4], nanoimprinting [5], solid state embossing [6], screen printing [7, 8], drop-on-demand (DOD) inkjet printing [9–12, 15–19] and laser induced forward transfer (LIFT) [13, 14], inkjet direct writing has emerged as an attractive direct patterning technique. This is chiefly because fully data driven and maskless drop-on-demand (DOD) inkjet processing is more versatile than other direct printing methods. Despite all its advantages, the resolution of the inkjet process is limited to the order of 20–50 μm [15, 16] and the material employed is typically a conducting polymer that has intrinsically high resistivity (two or three orders higher than metal) [15–17]. Although it is preferred to use metal electrodes and interconnects for high-quality transistor structures, high-resolution and low-temperature metal deposition methods that do not require photolithography or vacuum processes, are not yet well developed. This is because the material being printed should be in a viscous fluid state and metals have high melting temperatures making it difficult to obtain a material with the appropriate viscosity. Conducting polymers are not desirable for large-area or high-quality (high-speed) electronics [1, 18] even though they provide efficient electron injection into semiconducting polymers with small contact resistance [3]. Additionally, most of the direct writing techniques have demonstrated devices with a silicon wafer bulk gate, SiO_2 bulk dielectric layer and spincoated semiconductor in order to facilitate fabrication [9, 15–19]. However, this configuration is far from realizing practical flexible electronics and suffers from several problems such as large gate-to-source/drain overlap capacitance [1] and semiconductor leakage current [20]. Eventually, all patterned electronic components including gate and semiconductor active layer on polymer substrates will be required for the production of flexible electronics.

In this research, we demonstrate that selective laser sintering of inkjet printed metal nanoparticles enables low-temperature metal deposition as well as high-resolution patterning, thus overcoming the limitation of inkjet direct writing without any lithography processes. Combined with an air-stable carboxylate-functionalized polythiophene, all-inkjet-printed organic field effect transistors (OFETs) including a gate, dielectric layer and semiconductor layer with micron to submicron critical features by metal nanoparticle selective laser sintering were fabricated in a fully maskless sequence, eliminating the need for any lithographic processes. All processing and characterization steps were carried out at plastic-compatible low temperatures and in air under ambient pressure.

2. Fabrication and experimental details

Three different techniques were combined to achieve effective deposition of high-resolution metal patterns on a heat-sensitive, low-cost lightweight plastic substrate at low temperature and under ambient atmospheric pressure without using an expensive, toxic and time-consuming conventional lithographic process to realize low-cost and large-area flexible electronics. Firstly, the reduced processing temperature exploits the melting temperature depression of nanoparticles due to the thermodynamic size effect. Nanomaterials exhibit several interesting mechanical, chemical, optical and electrical properties that cannot be observed in their bulk counterparts due to the large surface to volume ratio, large surface energy and spatial confinement. Bulk gold starts to melt above 1063 °C. However, the melting temperature of the material drops to around 150 °C when the size of the nanoparticle shrinks under 2 nm due to the thermodynamic size effect [21]. The metal nanoparticles allow handling and treatment of metal components at a plastic-compatible low processing temperature in an inkjet based solution process without using any vacuum deposition method. Secondly, a focused laser beam was irradiated to deposit the energy and induce highly localized and efficient nanoparticle melting. Nanoparticle sintering could be done by applying an energy source such as a furnace or a laser beam. Local laser heating is advantageous due to the reduced heat-affected zone and more efficient energy deposition induced by the strong absorption peak generated by surface plasmon oscillation modes around a wavelength of 520 nm [22, 23]. This is in turn important for application on polymer substrates with low transition/melting temperature that are sensitive to blanket heating in a furnace or a heater. Laser sintered gold lines showed much greater uniformity and higher resolution (down to 1–2 μm) than those inkjetted and sintered by a heater ($\sim$100 μm) [10, 11]. Thirdly, inkjet printing of functional materials is used to deposit a nanoparticle suspension onto the substrate. The inkjet printing process delivers a vast range of functional materials with minimum waste and can be easily integrated with a CAD (computer aided design) system. The resolution of the conventional inkjet printing process is limited. However, combined with laser processing, the resolution could be enhanced to a level comparable to that of a lithographic process.

Figure 1 shows the basic concept of our approach. The metal nanoparticles are dispensed in organic carrier solvent and then inkjet printed on a polymer substrate to form nanoparticle

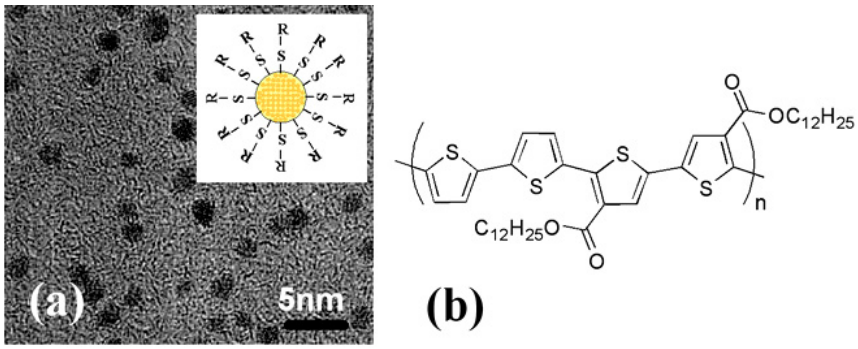

Figure 2. (a) A TEM image of SAM protected Au nanoparticles. The inset shows the schematics of a Au nanoparticle with SAM. (b) Chemical structure of modified polythiophene containing electron-withdrawing alkyl carboxylate substituents for enhanced air stability.

micro patterns (figure 1(a)). The inkjet printed nanoparticles are dried and then locally sintered by scanning with a focused Ar ion laser (514.5 nm wavelength, figure 1(b)). Finally, loosely bonded unsintered nanoparticles are simply washed away in an organic solvent to expose micro metal conductor structures (figure 1(c)). Based on the selective laser sintering of inkjet printed nanoparticles, high-resolution metal conductor patterns are fabricated and used for transistor gate/source/drain electrodes for transistors. Polymer dielectric layer and air-stable semiconducting polymer are inkjet printed to complete the OFET fabrication process.

2.1. Nanoparticle solution preparation

The gold nanoparticles protected by a self-assembled monolayer (SAM) were prepared by a two-phase reduction method reported by Hostetler *et al* [24]. Aqueous metal salts ($HAuCl_4$) were mixed in toluene solution containing long-chain alkylammonium surfactants to form a two-phase system. 1.5 g of tetroactylammonium bromide ($C_{32}H_{68}BrN$) was mixed with 80 ml of toluene and added to 0.31 g of hydrogen tetrachloroaurate (III) hydrate ($HAuCl_4{:}xH_2O$) in 25 ml of deionized (DI) water. Vigorous stirring transferred the metal salt ($AuCl_4^-$) into the organic phase (toluene) and the aqueous phase was removed. A measured quantity of capping agent, a long-chain thiol (hexanethiol), was added to the gold solution while stirring. Then, a reducing agent, sodium borohydride ($NaBH_4$), mixed in 25 ml of water was added into the organic phase by fast addition over approximately 10 s to nucleate nanocrystals. The mixture reacted at room temperature for 3.5 hours. The toluene was removed with a rotary evaporator and the leftover black particles suspended in ethanol and sonicated briefly. The particles were washed with ethanol and acetone and air dried. Monolayer-protected gold nanoparticles are suspended in alpha-terpineol at 10 wt%. SAM is critical for nanoparticles because it controls the size of the nanoparticles in addition to enhancing long-term stability and achieving favourable optical properties through Au–thiol chemistry. The size of the synthesized nanoparticles is distributed between 1 and 3 nm as measured by transmission electron microscopy (TEM) (figure 2(a)).

2.2. Semiconducting polymer preparation

The polymer (figure 2(b)) chosen for this study is a polythiophene derivative that has been shown to be more air stable than common organic semiconductors such as poly(3-hexylthiophene) (P3HT) [25]. The polythiophene derivative contains electron-withdrawing substituents that lower the highest occupied molecular orbital (HOMO) energy level of the polymer thereby reducing the level of p-doping by ambient oxygen. The sensitivity of conventional organic semiconducting polymers to air necessitates severe precautions during processing of semiconducting polymer material, device fabrication and characterization that are usually carried out either in a vacuum or a nitrogen environment. However, an air-free environment adds to the cost of manufacturing, thus offsetting advantages of the hybrid inkjet direct writing process that is meant to eliminate vacuum requirements. The air-stable semiconducting polymer used in this research is a novel material of a modified polythiophene containing electron-withdrawing alkyl carboxylate substituents, exhibiting high charge mobility. Due to the electron-withdrawing properties of the carboxylate substituents, the polymer has lower HOMO energy levels and therefore provides better oxidative doping stability than conventional solution-processible polythiophenes such as P3HT [25]. Semiconducting polymer was dissolved in warm (>45 °C) 1,2-dichlorobenzene (*o*-DCB) solvent (3 mg ml^{-1}) and inkjet printed as an active layer.

All chemicals were purchased from Aldrich and used without further purification unless otherwise noted. All solvents were purified on a solvent purification system. The reactions were performed under N_2 unless otherwise noted. All extracts were dried over anhydrous $MgSO_4$ and solvents were removed by rotary evaporation with vacuum assist. Flash chromatography was performed using Merck Kieselge l60 (230–400 mesh) silica. Detailed information on the semiconducting polymer can be found in [25].

2.3. Organic field effect transistor fabrication process and characterization (inkjet printing of nanoparticle solution, polymer dielectric layer and semiconducting polymer)

The organic field effect transistor (OFET) fabrication process consists of inkjet printing of functional materials (metal nanoparticle, polymer dielectric and semiconducting polymer) and subsequent thermal treatment by a scanning focused Ar ion laser. The OFETs fabricated in this work have a typical bottom gate/bottom contact transistor configuration wherein

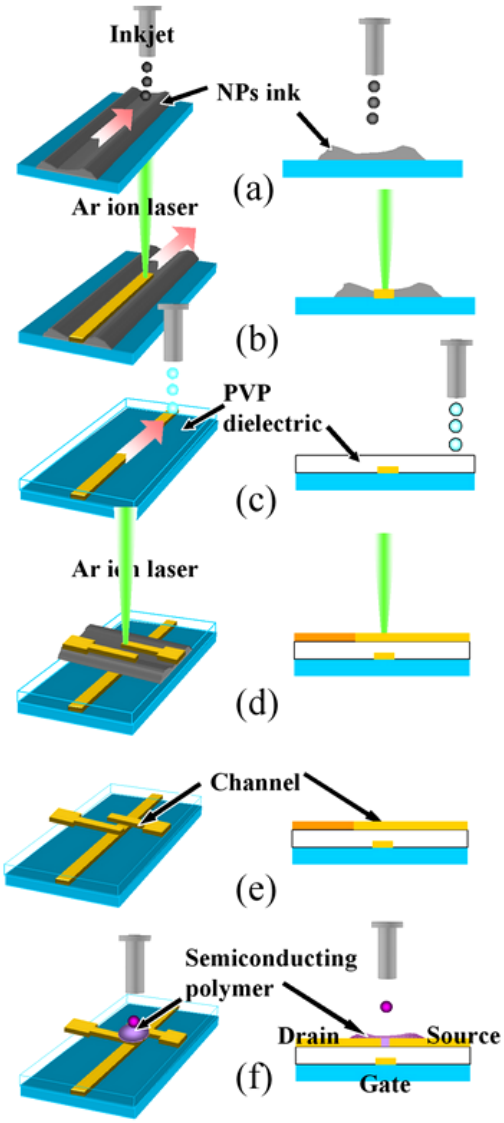

Figure 3. Process steps for OFET fabrication by laser selective sintering of a metal nanoparticle solution. (a) The nanoparticle solution is inkjet printed on plastic (exhibiting the ring stain problem). (b) A focused Ar ion laser beam scans the printed nanoparticles and selectively induces sintering to form a conductor pattern. (c) Washout of unsintered nanoparticles and inkjet printing of the PVP dielectric layer. (d) Inkjet printing of another nanoparticle solution line on top of the PVP layer and scanning a focused Ar ion laser beam to define source and drain electrodes. (e) Washout of unsintered nanoparticles to expose selectively sintered electrodes. (f) Inkjet printing and thermal annealing of semiconducting polymer at the channel.

the channel length is defined by the separation distance between two laser sintered conductor lines.

Figure 3 shows the detailed process steps for the OFET fabrication by laser sintering of inkjet printed metal nanoparticle solution on a polymer substrate (UPILEX-S, 25 μm thick, UBE Industries). A gate electrode was inkjet printed (figure 3(a)) by a piezoelectrically driven drop-on-demand (DOD) micro capillary tube (MicroFab, 50 μm nozzle diameter) and then selectively sintered (figure 3(b)) by scanning a focused Ar ion laser beam (514.5 nm, 3 kW cm^{-2}, beam diameter ($1/e^2$) $\sim$ 3.5 μm). The unsintered nanoparticles were then washed out to leave a narrow defined width gate. This narrow width gate reduces the geometric overlap capacitance between gate and source–drain electrodes, hence increasing the transistor switching speed [1, 17]. Then, 1.08 g poly-4-vinylphenol (PVP; MW $\sim$8000 AMU) dissolved in 15 ml hexanol with 0.1 ml cross-linking agent (poly(melamine-co-formaldehyde)), was inkjet printed on top of the gate line and cross-linked at 150 °C (figure 3(c)). The PVP jetting parameters and drop-to-drop spacing were carefully chosen. When the drop-to-drop spacing was excessive or too small, discontinuous lines were formed. At room temperature, the optimum drop-to-drop spacing was found to be about 100 μm. The jetting parameters of the bipolar voltage waveform were $\pm$15 V, 40 μs expansion and 80 μs contraction dwell time. Subsequently, another nanoparticle micro-line, which ultimately forms source and drain electrodes by selective laser sintering, was inkjet printed on top of the dielectric layer. A focused Ar ion laser beam was scanned along an inkjet printed line twice to write two parallel high-resolution electrodes by selective laser sintering (figure 3(d)). The bright parts represent the gold nanoparticles that were selectively sintered by the laser, and the dark parts indicate the unsintered gold nanoparticles. After selective laser sintering, the remaining unsintered nanoparticle was washed away in organic solvent exposing the two laser sintered parallel lines (figure 3(e)). These lines form the source and drain electrodes. The channel size can be controlled by varying the separation of these lines. As a last step, after laser sintering and washing out, the air-stable carboxylate-functionalized polythiophene semiconducting polymer was inkjet printed on the channel (figure 3(f)) and annealed at 120 °C on a hot plate for 3 min (figure 3(a)-(vi)). The patterned active area helps to reduce the gate bias induced leakage current and the drain current offset [20]. The thicknesses of the OFET layers are 25 μm (polymer substrate)/50–80 nm (gate, source, drain gold electrode)/380 nm (PVP dielectric)/100 nm (semiconducting polymer).

The device output and transfer characteristics were measured in air using a HP4155A semiconductor parameter analyzer and a probe station with the micro-positioning manipulators in a dark Faraday cage.

3. Results and discussion

3.1. Nanoparticle sintering characterization

Figure 4 shows the nanoparticle sintering characteristics investigated at various temperatures. Electrical resistance (figure 4, diamond symbol), reflectivity of nanoparticle film (figure 4, top insets) and weight percentage (not shown here) changed dramatically around 130–150 °C where the SAM started to desorb and evaporate from the nanoparticles. The resistance showed a sharp drop around 150 °C. The SAM protected nanoparticles as seen in the TEM image (figure 4, bottom left inset, taken with a JEOL 3010) are electrical insulators before the sintering process starts. After SAM desorption, the bare nanoparticles start to grow or form connected paths as a result of neck formation between particles (TEM image, figure 4, bottom right inset). The reflectivity

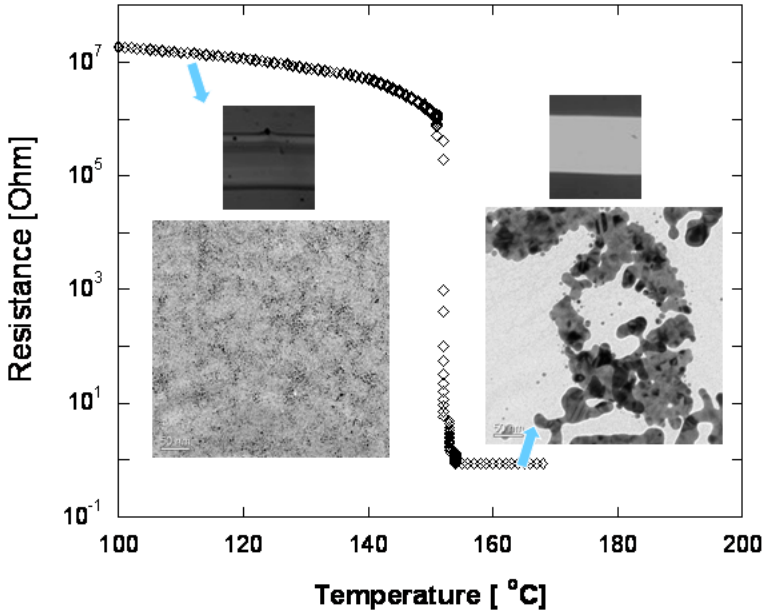

Figure 4. Resistance transient during the nanoparticle sintering process. Left column insets are a micrograph (top inset) and a TEM image on a carbon grid (bottom inset) of the unsintered nanoparticles. Right column insets are a micrograph (top inset) and a TEM image on a carbon grid (bottom inset) of the sintered nanoparticles. TEM images are at the same scale (inset scales correspond 50 nm). Note that although the electrical data are from a line written on a polymer substrate, the TEM images of the nanoparticle deposit are taken on a TEM carbon grid, prior to and after laser sintering in order to clarify the associated structural change.

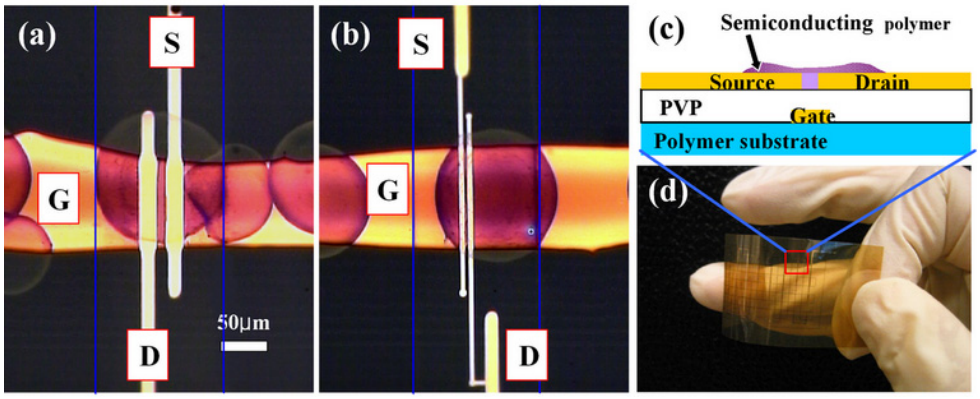

Figure 5. Micrographs of an OFET test structure with (a) a longer channel ($L \sim 10\ \mu$m) and (b) a shorter channel ($L \sim 1.5\ \mu$m). 'S', 'D' and 'G' indicate source, drain and gate, respectively. The circles are inkjet printed semiconducting polymer. The two bright vertical parallel lines are laser sintered gold electrodes (source and drain). The horizontal line is a gate electrode and is under the dielectric layer. The lines indicate the edges of an original inkjet printed line. (c) Schematics of an OFET. (d) Micrograph of arrays of OFETs fabricated on a polyimide substrate.

of the nanoparticle film increased and the color changed from black (figure 4 (top left inset)) to golden (figure 4 (top right inset)). In addition, TGA (thermogravimetry analysis) verified that about 17% of the mass loss (measured at 5 °C min^{-1} with a Seiko Instruments SSC 5200 TG/DTA 220 in an air environment) started to occur at almost the same temperature range. This 17% mass loss matches well with the theoretical mass percentage of the SAM on gold nanoparticles of diameter 3 nm. This temperature signifies that the nanoparticles start to sinter to form electrical conductors from the insulator.

3.2. OFET characterization

The transistors have a typical bottom gate/bottom contact configuration (figure 5(c)). Figures 5(a), (b) show micrographs of a single OFET with a narrow channel (figure 5(a), $L \sim 1.5\ \mu$m) and with a long channel (figure 5(b), $L \sim 10\ \mu$m). Two vertical bright lines are the source and drain electrodes. The separation gap between the two electrodes is a transistor channel. The underlying horizontal wide line is a gate line. The gate line and source/drain electrodes are separated by a thin transparent inkjet printed dielectric layer. The circular features represent inkjet printed and thermally annealed semiconducting polymer deposits. The two vertical lines indicate the edges of the original inkjet printed line. Note the reduction of feature size by selective laser sintering and the short channel production without any damage to the plastic substrate or the polymer dielectric layer by the nanoparticle selective laser sintering. The original inkjet printed line

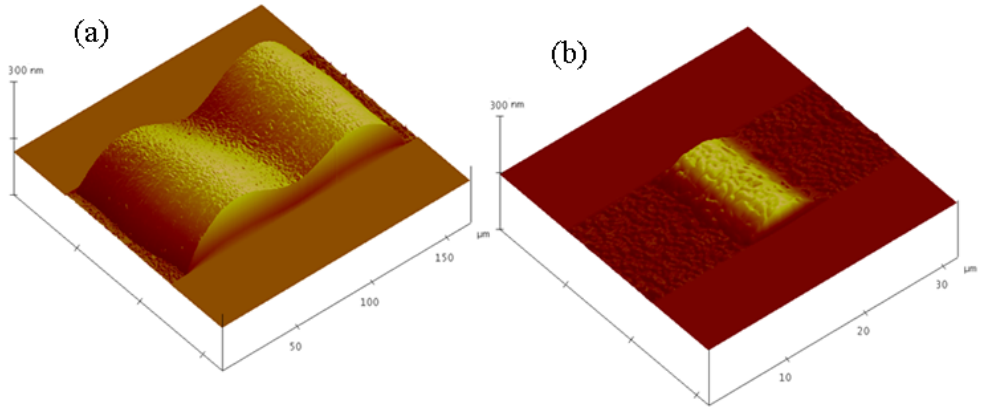

Figure 6. (a) AFM topographic images of (a) an original inkjet printed nanoparticle line (width $\sim$ 100 μm) and (b) a selectively laser sintered line (width $\sim$ 6 μm). The AFM images have the same height scale (300 nm) but a different lateral scale ((a) 170 μm $\times$ 170 μm, (b) 32 μm $\times$ 32 μm).

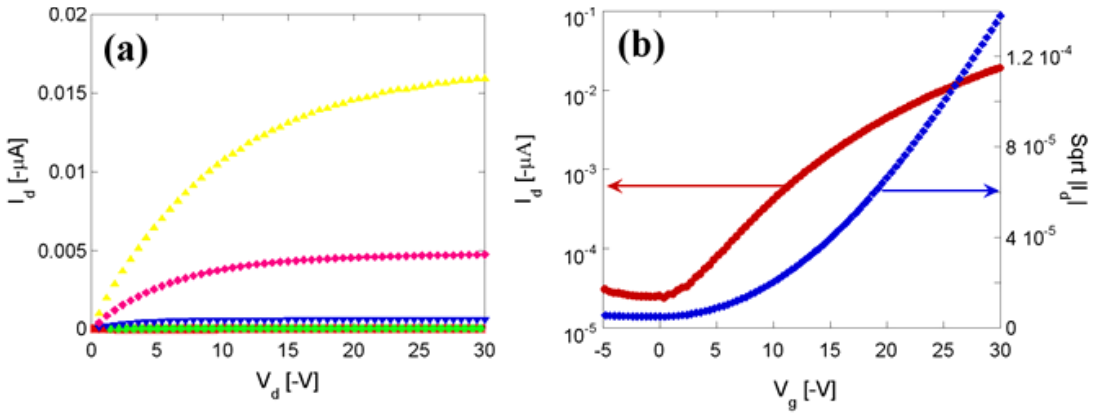

Figure 7. (a) Output and (b) transfer characteristics of OFETs by selective laser sintering of nanoparticles with air-stable polymer semiconductor ($L \sim 17$ μm, $W \sim 800$ μm). Output characteristics were measured for various gate voltages ($V_g = -30, -20, -10, 0, 10$ V) and transfer characteristics was measured at fixed drain voltage ($V_d = -30$ V).

shows a high rim structures at both edges (figure 6(a), AFM picture) due to the ring stain problem [26]. This highly non-uniform structure may cause shorting in the OFET multilayer. This problem can be alleviated by selective laser sintering of the central uniform part of the inkjet printed nanoparticle line (figure 6(b), AFM picture) and washing out the leftover high rim structure. Besides enhancement of uniformity, the resolution enhancement is obvious from the AFM pictures (figure 6). The selectively laser sintered nanoparticle line produces a conductor line several microns wide while the original inkjet printed line has a line width of $\sim$100 μm. Figure 5(d) shows how flexible the OFET array is on the polyimide substrate. The OFETs on a polymer substrate still work properly when bent to sub-centimeter radius.

The transfer and output characteristics of the OFETs on a plastic substrate with an inkjet printed and laser sintered gate, fabricated by selective laser sintering, are shown in figure 7. The transistor characteristics were measured in air using a HP4155A semiconductor parameter analyzer and a probe station with micro-positioning manipulators in a dark Faraday cage. For measurement of the output characteristics (figure 7(a)), the drain voltage (V_d) was scanned from 0 to -30 V and the drain current (I_d) was measured while the gate voltage (V_g) was fixed at -30, -20, -10, 0 and 10 V during each V_d scanning. For the measurement of transfer characteristics (figure 7(b)), the gate voltage (V_g) was scanned from 5 to -30 V and the drain current (I_d) was measured while the drain voltage (V_d) was fixed at -30 V. The OFET has a 17 μm wide (L) and 800 μm long (W) channel. Selectively laser sintered OFETs showed typical output and transfer characteristics with operation in p-type accumulation mode with a hole mobility of 0.002 cm^2 V^{-1} s^{-1}, an I_{on}/I_{off} ratio of 10^3–10^4 and turn voltage of around -12 V. When the channel size shrinks to less than 6 μm, the OFETs exhibited output characteristics without current saturation or even superlinear dependence for shorter channels with less mobility and similar I_{on}/I_{off} ratio. Over time, a negative shift in the threshold voltage was observed. Devices were therefore subjected to a positive gate and source–drain voltage ($V_g = +30$ V, $V_d = 0$ to $+30$ V) before operation to investigate whether the original threshold voltages could be recovered by reducing traps that could have formed within the film [25].

For verification of the current process, a standard FET sample was fabricated by a lithographic technique. A p+ silicon wafer was oxidized by wet oxidation for 37 min at 900 °C to grow a 115 nm SiO_2 dielectric layer. The gold

electrode was patterned by a lift-off technique using directional gold deposition. The semiconducting polymer was deposited under the same condition for inkjet printed and laser sintered samples. The overall performance of the lithographically processed OFET with a SiO_2 dielectric layer was similar to that of the laser-fabricated OFETs. This result could verify that, besides several advantages, the direct writing process laid out in this work yields devices of as good quality as those obtained by a conventional lithographic process.

All-inkjet-printed OFETs via direct writing are attractive since they are compatible with large-area, cost-effective processes. However, gate and dielectric layer inkjet printing are challenging because inkjet printed gate lines face the non-uniformity problem caused by the ring stain phenomenon [26]. Therefore, the dielectric layer shows leakage current problems due to gate–source/drain shorted circuit, cracks, pin-holes and defects [27]. A thick dielectric layer could be a potential solution for working capacitors but will decrease the capacitance, requiring increased turn-on voltage for transistor operation. A focused laser beam can produce high resolution and uniform gate lines by selective sintering at the central part of the inkjet printed nanoparticle and by washing out unsintered high rim structures (figure 6). The dielectric layer alignment problem could be solved by deliberately altering the surface characteristics. A PVP dielectric layer was inkjet printed along the gate line and the self-alignment process facilitated perfect dielectric layer coverage of the underlying gate line due to the higher wettability of the high-energy metal gate than the lower-energy glass or polymer substrate [28].

The performance of the transistors can be significantly enhanced by the following approaches. First, further shrinking of the critical channel dimension can be accomplished by an alternative high-resolution subtractive method. Recently, we also demonstrated that short pulsed laser radiation can ablate nanoparticle films to define submicron channels on a polymer substrate [29]. By ablating unsintered nanoparticle films, clean and precise patterning characterized by a low ablation threshold could be achieved. The resolution of selective laser sintered OFETs is determined by heat diffusion, which is a sensitive function of several parameters including the laser spot size, energy, scanning speed and film thickness. It is difficult to fabricate very short channels (<5 μm) in a reliable and reproducible fashion. On the other hand, the resolution of selective laser ablated and sintered OFETs is more dominated by the laser spot size than by other parameters as long as the laser pulse energy is above the threshold, hence increasing the reliability and predictability of the process. Along with the metal nanoparticle selective laser sintering method, short pulsed laser ablation is a promising approach for submicron high-resolution transistor fabrication and is under investigation in this laboratory. Secondly, the contact limited device characteristics can be further improved by proper choice of the nanoparticles in terms of matching the workfunction with the semiconducting polymer. Carboxylate-functionalized polythiophenes exhibit a relatively high ionization potential (HOMO $\sim$ -5.84 eV, bandgap $\sim$ 2.35 eV), which makes them less prone to doping by ambient oxygen but results in a considerable contact effect. It has been reported that in bottom contact polymer transistors with a relatively large Schottky barrier for hole injection ($\phi_b > 0.3$ eV), the source contact resistance is considerably larger than the drain contact resistance and is dominated by charge-carrier injection at the source [30]. This effect is more pronounced for OFETs with channels shorter than the critical channel length ($L_c \sim 6$ μm). Other metal nanoparticles (Ag, Cu, Al etc) can be utilized because our processing method is certainly not exclusive to gold. The critical channel length can be reduced and the contact-limited output-device characteristics can be further improved by proper choice of the nanoparticles in terms of workfunction matching with the semiconducting polymer. Thirdly, semiconducting materials with higher mobility and different transistor structures such as top gate configuration can be applied due to the great flexibility in the material choice of the current inkjet printing process.

4. Summary

All-printed electronics is the key technology to ultra-low-cost electronics such as radiofrequency identification devices and large-area displays. As a critical step in this direction, air-stable OFETs were fabricated using inkjet printing and low-temperature selective laser sintering. OFET electrodes having great resolution and highly electrically conductive gold lines were fabricated in ambient pressure and at room temperature without using any lithographic process. To overcome the shortcomings of conventional organic semiconducting polymers and maintain the great advantage of the inkjet direct writing process, carboxylate-functionalized polythiophene with increased air stability was used as the semiconducting material for OFETs fabricated by a laser sintering process. The OFETs showed good and typical accumulation mode p-channel transistor behaviour with a carrier mobility of 0.002 $cm^2\ V^{-1}\ s^{-1}$ and a I_{on}/I_{off} ratio ranging from 10^3 to 10^4. The OFET performance can be enhanced by further shrinking of the channel dimension and by applying other metal nanoparticles and semiconducting polymers. This maskless and direct writing process can contribute to the development of inexpensive and large-area macro-electronics. Furthermore, the local material deposition of the inkjetting process could minimize material waste. Local thermal control of the laser sintering process could confine the heat-affected zone and help avoid thermal damage to the substrate.

Acknowledgments

The authors wish to thank Professor Vivek Subramanian of the Department of Electrical Engineering and Computer Sciences, University of California, Berkeley for valuable discussions. Financial support to the University of California, Berkeley by the US National Science Foundation under grant CTS-0417563 and CMMI 0700827, the Department of Energy (DE-AC03-76SF00098), and to the Swiss Federal Institute of Technology in Zurich by the Swiss National Science Foundation under grant no. 2000-063580.00 is gratefully acknowledged.

References

[1] Zschieschang U, Klauk H, Halik M, Schmid G and Dehm C 2003 *Adv. Mater.* **15** 1147–51
[2] Redinger D, Molesa S, Yin S, Farschi R and Subramanian V 2004 *IEEE Trans. Electron Devices* **51** 1978–83
[3] Loo Y L, Someya T, Baldwin K W, Bao Z, Ho P, Dodabalapur A, Katz H E and Rogers J A 2002 *Proc. Natl Acad. Sci.* **99** 10252–6
[4] Zaumseil J, Someya T, Bao Z, Loo Y L, Cirelli R and Rogers J A 2003 *Appl. Phys. Lett.* **82** 793–5
[5] Ko S H, Park I, Pan H, Grigoropoulos C P, Pisano A P, Luscombe C K and Fréchet J M J 2007 *Nano Lett.* **7** (doi:10.1021/nl070333v)
[6] Stutzmann N, Friend R H and Sirringhaus H 2003 *Science* **299** 1881–4
[7] Ganier F, Hajlaoui R, Yasser A and Srivastava P 1994 *Science* **265** 1684–6
[8] Bao Z, Feng Y, Dodavalapur A, Raju V R and Lovinger A J 1997 *Chem. Mater.* **9** 1299–301
[9] Ridley B A, Nivi B and Jacobson J M 1999 *Science* **286** 746–9
[10] Chung J, Ko S, Bieri N R, Grigoropoulos C P and Poulikakos D 2004 *Appl. Phys. Lett.* **84** 801–3
[11] Chung J, Bieri N R, Ko S, Grigoropoulos C P and Poulikakos D 2004 *Appl. Phys.* A **79** 1259–61
[12] Wang J Z, Zheng Z H, Li H W, Huck W T S and Sirringhaus H 2004 *Nat. Mater.* **3** 171–6
[13] Piqué A, Chrisey D B, Fritz-Gerald J M, McGill R A, Auyeng R C Y, Wu H D, Lakeou S, Nguyen V, Chung R and Duiganan M 2000 *J. Mater. Res.* **15** 1872–5
[14] Tan B, Venkatakrishnan K and Tok K G 2003 *Appl. Surf. Sci.* **207** 365–71
[15] Sirringhaus H, Kawase T, Friend R H, Shimoda T, Inbasekaran M, Wu W and Woo E P 2000 *Science* **290** 2123–6
[16] Sirringhaus H and Shimoda T 2003 *MRS Bull.* **28** 802–6
[17] Sele C W, Werne T V, Friend R H and Sirringhaus H 2005 *Adv. Mater.* **8** 997–1001
[18] Burns S E, Cain P, Mills H, Wang J and Sirringhaus H 2003 *MRS Bull.* **28** 829–34
[19] Ko S, Pan H, Luscombe C, Fréchet J M J, Grigoropoulos C P and Poulikakos D 2007 *Appl. Phys. Lett.* **90** 141103
[20] Jia H, Pant G K, Gross E K, Wallace R M and Gnade B E 2006 *Org. Electron.* **7** 16–21
[21] Buffat P A and Borel J P 1976 *Phys. Rev.* A **13** 2287–98
[22] Bohren C F and Huffman D R 1983 *Absorption and Scattering of Light by Small Particles* (New York: Wiley)
[23] Antoine R, Brevet P F, Girault H H, Bethell D and Schiffrin D J 1997 *Chem. Commun.* **19** 1901–2
[24] Hostetler M J *et al* 1998 *Langmuir* **14** 17–30
[25] Murphy A R, Liu J, Luscombe C, Kavulak D, Fréchet J M J, Kline R J and McGehee M D 2005 *Chem. Mater.* **17** 4892–9
[26] Deegan R D, Bakajin O, Dupont T F, Huber G, Nagel S R and Witten T A 1997 *Nature* **389** 827–9
[27] Wallace D B, Cox W R and Hayes D H 2002 *Direct-Write Technologies for Rapid Prototyping Applications* (New York: Academic)
[28] de Gennes P G, Brochard-Wyart F and Quere D 2004 *Capillarity and Wetting Phenomena* (New York: Springer)
[29] Ko S, Choi Y, Hwang D J, Grigoropoulos C P and Poulikakos D 2006 *Appl. Phys. Lett.* **89** 141126
[30] Bürgi L, Richards T J, Friend R H and Sirringhaus H 2003 *J. Appl. Phys.* **94** 6129–39